

Received: 2018.08.14  
Accepted: 2018.10.01  
Published: 2018.11.27

# P27 Protects Cardiomyocytes from Sepsis via Activation of Autophagy and Inhibition of Apoptosis

Authors' Contribution:  
Study Design A  
Data Collection B  
Statistical Analysis C  
Data Interpretation D  
Manuscript Preparation E  
Literature Search F  
Funds Collection G

ABF 1 **Xianyuan Zhao\***  
DFG 2 **Hong Qi\***  
ABG 3 **Jiamin Zhou**  
CDE 4 **Shuqi Xu**  
CDE 1 **Yuan Gao**

1 Department of Critical Care Medicine, Renji Hospital, School of Medicine, Shanghai Jiaotong University, Shanghai, P.R. China  
2 Department of Traditional Chinese Medicine, Renji Hospital, School of Medicine, Shanghai Jiaotong University, Shanghai, P.R. China  
3 Department of Hepatic Surgery, Shanghai Cancer Center, Fudan University, Shanghai, P.R. China  
4 Department of Gastroenterology, Shidong Hospital, Anhui University school of Medicine, Hefei, Anhui, P.R. China

\* Xianyuan Zhao and Hong Qi contributed equally to this work and should be considered as equal first coauthors

Yuan Gao, e-mail: gaoyuanzhuren@aliyun.com

**Corresponding Author:**  
**Source of support:**

Departmental sources

**Background:** It has been reported that p27Kip1 plays an important role not only in the inhibition of cyclin-dependent kinases but also in the regulation of autophagy under various metabolically related stress conditions, including glucose deprivation and endoplasmic reticulum stress. However, its effect on lipopolysaccharide (LPS)-induced cardiomyocyte stress *in vitro* remains unclear. Here, we measured the increased expression of LC3-II and visualized autophagosomes *in vitro* by immunofluorescent assays after treatment with a p27 fusion protein.

**Material/Methods:** Cardiomyocyte contractile properties were assessed by measuring cell shortening and re-lengthening. Apoptosis was evaluated by terminal deoxynucleotidyl transferase dUTP nick end labeling (TUNEL) staining. Western blot, colorectal ligation puncture (CLP) surgery, silencing of Atg5 expression by small interfering RNA (siRNA), and immunofluorescent assays were also performed in this study.

**Results:** After exogenous delivery of the p27 fusion protein and overexpression of p27 in LPS-induced cardiomyocytes, we found lower expressions of caspase-3 and caspase-8 and reduced positive TUNEL staining. Improved cardiomyocyte mechanical functions and reduced apoptosis were diminished after treatment with various autophagy inhibitors. Intravenous injections of p27-expressing adeno-associated virus serotype 9 (AAV9) vectors resulted in cardiac specific overexpression of p27, and echocardiography was used to assess cardiac function and structure in sepsis rat models. We observed improved cardiac function and reversed adverse ventricular remodeling after the introduction of AAV9 vectors. Meanwhile, apoptosis was reduced, and expression of LC3-II was elevated in septic rat models treated with AAV9 vectors compared to controls.

**Conclusions:** The study data demonstrated that the overexpression of p27 protects cardiomyocytes from sepsis-induced cardiac depression via the activation of autophagy and inhibition of apoptosis.

**MeSH Keywords:** **Asepsis • Sepsis • Systemic Inflammatory Response Syndrome**

**Full-text PDF:** <https://www.medscimonit.com/abstract/index/idArt/912750>



3779



5



34



## Background

Numerous studies have demonstrated that p27 plays an important role in regulating G0/G1 cell-cycle arrest and maintaining quiescence, and hence, p27 has been deemed as a canonical tumor suppressor [1,2]. Thus, p27 inhibits cell proliferation and organ enlargement via inhibition of cyclin-dependent kinases (CDK), and it is regarded as a proliferative inhibitor and a gatekeeper of cell cycle entry in various malignant tumors [1,2]. However, in recent years, several non-canonical biological functions have been reported, including cell migration, regulation of autophagy, and cytoskeletal dynamics via CDK-independent signaling pathways [3–6]. The phosphorylation of p27, induced by the activation of the LKB1-AMPK signaling pathway in breast cancer cells, stabilized p27 and promoted cell survival in malnutrition conditions by improving the autophagic flux, which demonstrated that p27 could regulate autophagy and improve cell survival under stress conditions [7]. Furthermore, p27 depletion in MCF-7 cells enhanced apoptosis in a manner not related to the regulation of cell-cycle progression [7]. More intriguingly, p27 also protected cardiomyocytes from apoptosis via the activation of autophagy after glucose deprivation [8]. In addition to the inhibition of cell proliferation, these novel studies demonstrated intricate functions for p27, including autophagy regulation and cell survival in cells such as cardiomyocytes and cancer cells, which suggests that p27 may be involved in pathophysiological processes in various diseases.

In other environmental stress conditions, including systemic inflammation *in vivo* or LPS-induced cell stress *in vitro*, the cytoprotective functions of p27, as observed in metabolically stressed models, are still unexplored. Septic animals in colorectal ligation puncture (CLP) models are characteristic of multiple organ dysfunction syndrome (MODs) and even multiple organ failure (MOF), including impaired cardiac contractile dysfunction and cardiomyocyte apoptosis via Toll-like receptor 4 (TLR4)/nuclear factor kappa-B (NF- $\kappa$ B) signaling and oxidative stress. In clinical epidemiologic surveys, the presence of cardiac dysfunction in septic patients showed significantly increased mortality, by 70–90%, compared to patients without cardiac depression [9]. However, the mechanism of cardiac depression in septic patients or septic animal models is rather complicated. According to previous studies, the production of myocardial depressant substances and aberrant release of pro-inflammatory cytokines may be the main factors resulting in cardiac dysfunction [10,11]. More recent studies have demonstrated that autophagy is involved in cardiac contractile dysfunction in sepsis models, and an impairment of autophagy may contribute to cardiac depression and the death of cardiomyocytes [12,13]. Studies have shown that in the early stage of sepsis, the autophagic flux increased because of the increased expression of Beclin1 at 8 hours, whereas it

was significantly decreased at 24 hours after CLP, which demonstrated that the impairment of autophagy flux occurred in the late stages of sepsis; however, rapamycin could reverse depressed cardiac contractile function in the late stages of sepsis by the complete induction of autophagic flux [14,15]. *In vitro*, apoptosis occurred as soon as autophagy returned to baseline levels after 24 hours of treatment with lipopolysaccharide (LPS), and silencing of *ATG5* with specific small interfering RNA (siRNA) molecules accelerated cardiomyocyte apoptosis after the introduction of LPS via the inhibition of autophagy [14].

In the present study, we hypothesized that the dysfunction of autophagy could be restored by exogenously supplementing with p27 protein in cardiomyocytes treated with LPS, and we found that the enhanced autophagy protected cardiomyocytes from sepsis and inhibited apoptosis *in vivo* and *in vitro*. These data suggest that p27 could be a potential therapeutic target in sepsis-induced cardiac depression and hemodynamic disturbances.

## Material and Methods

### Isolation of primary cardiomyocytes and cell culture

Primary cardiomyocytes from neonatal Wistar rats were isolated according to previously described protocols [16]. The hearts were removed, cut into pieces, and then enzymatically digested with Liberase TH (2.5  $\mu$ g/mL; Roche, Switzerland) and pancreatin (1 mg/mL; Sigma) in Hank's balanced salt solution as previously described. The supernatant was then added to complete Dulbecco's modified eagle medium (DMEM). Then 2  $\mu$ L of dilute enzymatic solution was added to continue digesting the remaining tissue after the cell suspension was removed. The final cell suspension was filtered twice through 70  $\mu$ m strainers and then plated in complete DME culture medium containing 10% fetal bovine serum and 1% penicillin/streptomycin. Trypan blue staining was used for the assessment of cell viability. The highly active cardiomyocytes were used for the measurement of mechanical properties as described. Every procedure was approved by the Animal Care and Use Committee of the Renji Hospital, Shanghai Jiao Tong University School of Medicine and was in conformity with the guidelines of National Institute of Health (No81004).

### Protein extraction and western blot

Proteins from cultured cardiomyocytes and hearts of septic rats were prepared in lysis buffer according to standard protocols. Equal amounts of protein were separated by SDS-PAGE and transferred onto a PVDF membranes (Millipore). Membranes were blocked with 5% milk in Tris-Buffered Saline Tween-20 (TBST) for 2 hours at 37°C and incubated overnight

at 4°C with the following primary antibodies: anti-LC3 (1: 500, ab56810, Abcam), anti-GAPDH (1: 1000, sc-47778, Santa Cruz Biotechnology), anti-caspase-8 (1: 1,000, 9504, Abcam), anti-caspase-3 (1: 1,000, 6992, Abcam). Membranes were washed and incubated with secondary antibody for 1 hour at 25°C. Chemiluminescence was used for the visualization of the blotted bands and the gray values of the protein bands were measured using the ECL Fuazon Fx (Vilber Lourmat).

### Colorectal ligation puncture (CLP) surgery

The CLP surgery was performed as previously described [17]. Rats were anesthetized with 10 mg/mL ketamine (Gutian Pharmaceuticals) and the cecum was 100% ligated with sterile 10 mm stainless steel surgical clips outside the abdominal cavity after exposure of the cecum site. The puncture was performed 3 times with a 22-gauge needle. The intestinal tube was repositioned outside the abdominal cavity and the abdominal cavity was closed with a 4-0 sterile suture. We opened the abdominal cavity only in sham-operated rats but without ligation and puncture at the site of the cecum.

### Immunofluorescent assays

For immunostaining, cardiomyocytes and heart sections from septic rats were fixed in 4% paraformaldehyde at 25°C for 10 minutes and then permeabilized with 0.01% Triton X-100 for 10 minutes at room temperature. Subsequently, the fixed cells were incubated with 5% bovine serum albumin for 30 minutes at 25°C. The cells were then treated with a rabbit polyclonal antibody against LC3 (1: 1500, ab58610, Abcam), used to measure the expression of LC3 in primary cardiomyocytes cells after induction with LPS. Further, the cells were incubated for 1 hour at 37°C with fluorescein isothiocyanate (FITC)-labeled anti-rabbit IgG (H+L) secondary antibody (072-01-15-06, KPL). Finally, the cells were visualized by confocal laser scanning microscopy (Leica, Wetzlar, Germany).

### TUNEL (terminal deoxynucleotidyl transferase dUTP nick end labeling)

TUNEL staining was performed as previously described. Apoptosis in cultured cardiomyocytes and heart tissues was assessed using the *In Situ* Cell Death Detection Kit (Roche, Mannheim, Germany) according to the manufacturer's instructions. In brief, the cells and tissue sections (3 sections per rat) were fixed in 4% paraformaldehyde at room temperature for 15 minutes and then the membranes and karyothecas were permeabilized with 0.01% Triton X-100 for 10 minutes at room temperature. After addition of the TUNEL reaction mixture, the sections were incubated for 60 minutes at 37°C. Subsequently, diphenyl phenylindole (DAPI) staining was performed to observe the cell nucleus. Finally, the cells and sections

were rinsed with phosphate buffered saline (PBS) buffer solution 3 times and visualized by confocal laser scanning microscopy (Leica, Wetzlar, Germany).

### Transfection of adeno-associated virus vectors

The construction of adeno-associated virus serotype 9 (AAV9) vector, characterized by partial cardiac specificity, encoding p27 and green fluorescent protein (GFP) was carried out by the Shanghai Jikai Gene Chemical Technology Co., Ltd. (China, Shanghai). The AAV9 vector was used for the overexpression of p27 in primary cardiomyocytes and in hearts of septic rats via intravenous injection at the jugular vein. The negative control was constructed using a scrambled sequence not capable of encoding the target protein. The protocol for transfection was performed according to the standard procedure as previously described. Primary cardiomyocytes were seeded on 24-well plates at a density of ~5000 cells/well and incubated at 37°C. On the second day, the cells were transfected with AAV9 vectors for 10 to 12 hours using Lipofectamine 2000 (Invitrogen) according to the standard manufacturer's instructions. The cells with green fluorescence indicated stable transfection with the AAV9-mediated vector. In total, >85% of cells were positive for green fluorescence as visualized by fluorescence microscopy, thereby indicating the successful establishment of cell models, classified as negative control and AAV9-p27 (overexpression), respectively. The green fluorescent signals in hearts observed by fluorescent microscopy indicated the establishment of p27 overexpression in heart tissues of septic rats as well.

### Silencing of *Atg5* expression by siRNA

Five nanomole siRNA specific for *Atg5* or scramble control (Invitrogen) was used to transfect cardiomyocytes using Lipofectamine 2000 (Invitrogen) according to the standard manufacturer's instructions after treatment with TAT-p27 and LPS. After 24 hours of siRNA incubation, cardiomyocytes were harvested to measure the expression of proteins related to apoptosis and mechanical properties.

### Measurements of cell shortening and re-lengthening

Mechanical properties of cardiomyocytes were assessed using the SoftEdge MyoCam system (IonOptix Corporation, Milton, MA, USA) as previously described [18]. In brief, cardiomyocytes were placed in a chamber equipped on platforms of an inverted microscope and incubated at 25°C with a buffer containing 131 mM NaCl, 4 mM KCl, 1 mM CaCl<sub>2</sub>, 1 mM MgCl<sub>2</sub>, 10 mM glucose, and 10 mM HEPES, at pH 7.4. The cells were stimulated with a suprathreshold voltage at a frequency of 0.5 Hz, for a 3 ms duration, which provokes muscle contractions (FHC Inc, Brunswick, NE, USA). The myocyte was visualized on a computer monitor using an IonOptix MyoCam camera.

The corresponding SoftEdge software was applied to monitor the changes in cell length during shortening and re-lengthening. Cell shortening and re-lengthening were assessed using the following indices: peak shortening (PS), maximal velocities of cell shortening and re-lengthening ( $\pm$ dL/dt), time-to-PS (TPS), and time-to-90% re-lengthening (TR90).

### Statistical analysis

All experiments were repeated at least 5 times and the data are presented as the mean  $\pm$  standard deviation (SD). Unpaired *t*-tests were used to determine the statistical differences between 2 groups in each analysis. A one-way analysis of variance (ANOVA) was used for multiple comparisons.  $P < 0.05$  was considered to be statistically significant. All data were analyzed by the log-rank test. All statistical analyses were performed with SPSS 13.0.

## Results

### Exogenous delivery of TAT-p27 and overexpression of p27 promoted autophagy in LPS-induced cardiomyocytes *in vitro*

To verify if p27 promotes autophagy when cultured cardiomyocytes are exposed to environmental stresses, including exposure to LPS, we exogenously delivered a p27 fusion protein (TAT-p27) and overexpressed p27 using AAV9 expressing the gene encoding human p27 in primary cardiomyocytes isolated from rats. We then measured the expression of microtubule-associated protein (LC3)-I and LC3-II, protein markers of autophagosomes, by western blot in *in vitro* experiments. We found that both the exogenous delivery of TAT-p27 and AAV-overexpression of p27 (AAV9-p27) in cardiomyocytes increased the expression of LC3-II (Figure 1A), a biomarker of active autophagosome formation, with an increase in the LC3-II/LC3-I ratio (Figure 1B), demonstrating that p27 promoted autophagy flux in LPS-induced cardiomyocytes. Furthermore, we performed immunofluorescent assays to detect the formation of LC3-II positive puncta during the process of autophagic flux. We found that p27 increased the accumulation of LC3-II positive puncta in LPS-induced cardiomyocytes after introduction of TAT-p27 or overexpression with AAV9-p27 (Figure 1C). These results demonstrate that p27 indeed promotes autophagy in cardiomyocytes after treatment with LPS.

### p27 suppressed apoptosis in cardiomyocyte treated with LPS *in vitro*

Autophagy is a highly conserved mechanism related to cell survival, and dysfunction of autophagy and low expression of p27 are considered to be involved in various forms of heart disease,

including heart failure and myocardial infarction [19–21]. In previous studies, Wu et al. found that recombinant p27 protein inhibited cardiac apoptosis and improved adverse remodeling after coronary artery occlusion [22]. Nakai et al. found that cardiac specific silencing of *Atg5* leads to increased apoptosis and a deteriorative cardiac function in basal and pressure overload conditions, which suggests that a deficiency in autophagy leads to the impairment of cell survival and promotion of apoptosis [23]. Therefore, we considered that p27 could also suppress apoptosis in LPS-induced cardiomyocytes according to these previous studies. We measured cleaved caspase-3 and caspase-8 in cardiomyocytes preconditioned with TAT-p27 and in non-preconditioned cardiomyocytes, used as a negative control, after treatment with LPS. We found that preconditioning with TAT-p27 reduced the expression of apoptosis-related proteins as expected (Figure 2A, 2B). Subsequently, we measured the number of TUNEL-positive cells in cardiomyocytes pretreated with TAT-p27 after exposure to LPS to measure the level of apoptosis. We found a decrease in the number of TUNEL-positive cells, which demonstrated that p27 inhibited apoptosis in LPS-induced cardiomyocytes (Figure 2C, 2D). To further investigate whether the enhanced autophagy contributed to the inhibition of apoptosis, we utilized different autophagy inhibitors, including bafilomycin A1, 3-methyladenine, and chloroquine to repress the autophagic flux and detect the apoptosis after administration of autophagic inhibitors. We observed that the utilization of all the autophagy inhibitors resulted in increased apoptosis compared to the absence of these inhibitors (Figure 2A–2D). These data demonstrate that p27 protected cardiomyocytes from apoptosis after exposure to LPS via the activation of autophagy.

### p27 improved cardiac mechanical contractile functions after treatment with LPS

Although numerous studies have reported that autophagy may play a role in the regulation of cardiac functions in various disease models and pathological conditions, the results have been inconsistent. The effect of autophagy on cardiac contractile function and cell death is still not clear in LPS-induced cardiomyocytes, even if autophagy was deemed as a protective factor in septic animal models and a vital cellular mechanism contributing to cell survival [24,25]. A previous study demonstrated that a deficiency in autophagic flux impaired the recovery of cardiac functions in ischemia-reperfusion injury, which suggested that autophagy may have a positive effect on cardiomyocytes exposed to cardiovascular stress [20]. To investigate and clarify the effect of p27 on cardiomyocytes stimulated by LPS, we performed an assessment of the mechanical properties in LPS-induced cardiomyocytes. We found that the exogenous delivery of p27, or overexpression of p27, did not change the resting cell length but improved mechanical contractile function (Figure 3A), represented by an increase in

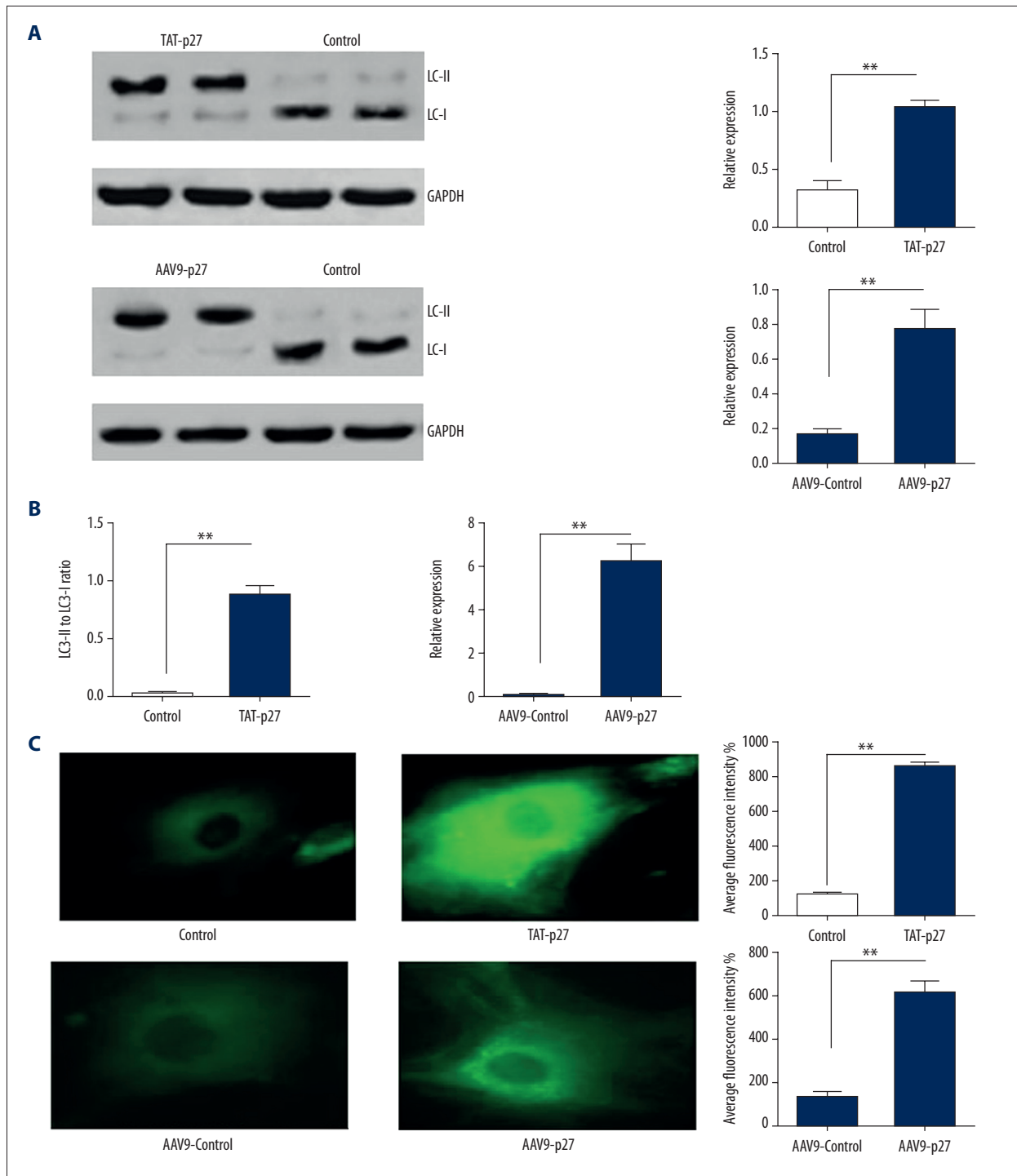


**Figure 1.** Administration of TAT-p27 and overexpression of p27 promote autophagy in LPS-induced cardiomyocytes *in vitro*. **(A)** Representative figures and quantitative analyses of immunoblots reflect the expression of LC3-I and LC3-II in LPS-induced primary cardiomyocytes with or without exogenous TAT-p27 and overexpression of p27 by the AAV9 vector. **(B)** The ratio of the relative expression of LC3-II to LC3-I (GAPDH used as a reference protein) in LPS-induced primary cardiomyocytes with or without exogenous TAT-p27 and AAV9-p27. **(C)** Representative figures and quantitative analyses of immunofluorescent assays of LC3-II in primary cardiomyocytes treated with exogenous TAT-p27, AAV9-p27, and negative control. The bright green puncta represent the formation of autophagosomes and the expression levels of LC3-II in primary cardiomyocytes. The experiments were replicated 3 times. Data are presented as the mean  $\pm$ SD. \*\*  $P < 0.01$ , \*  $P < 0.05$ .

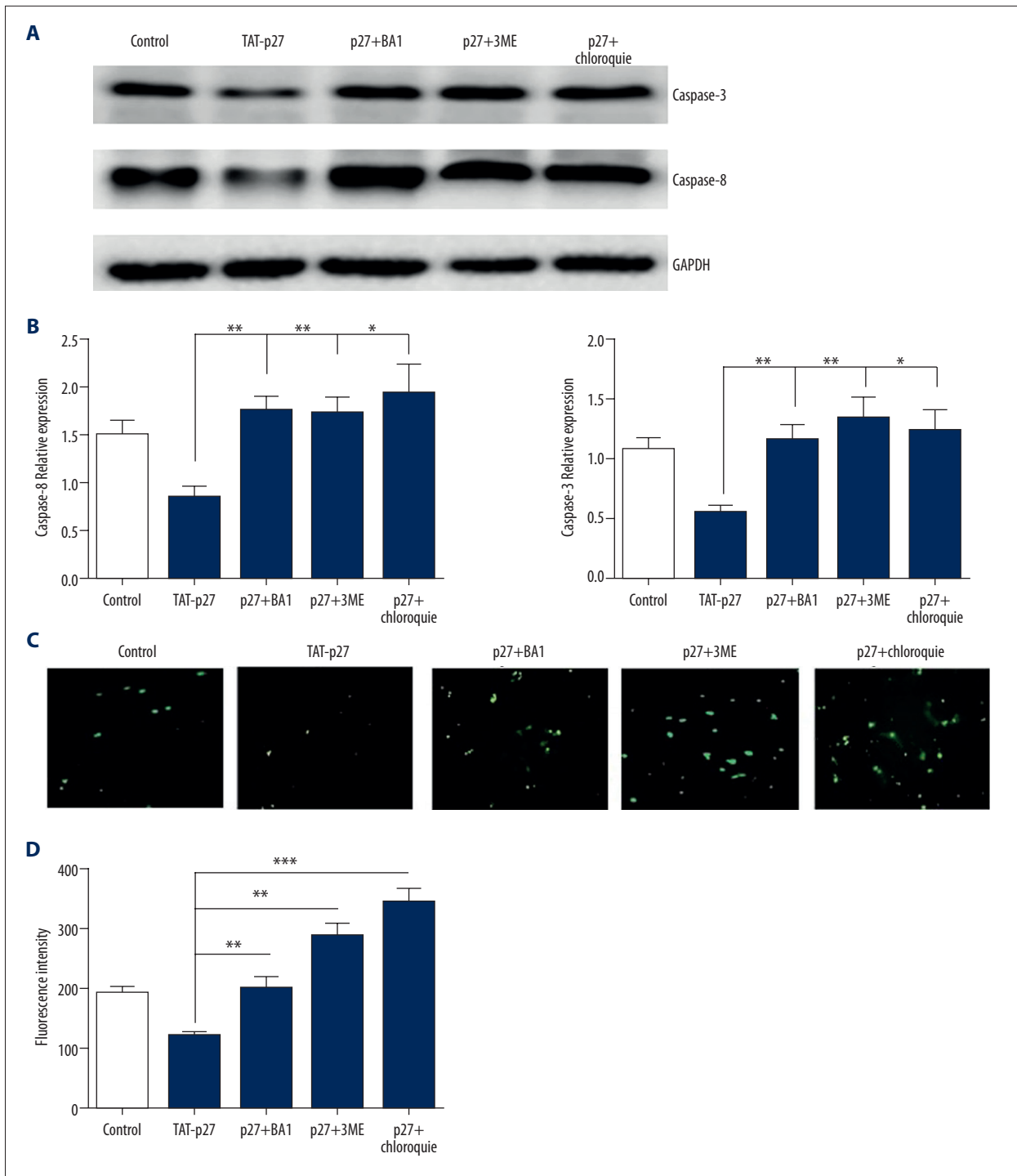


**Figure 2.** Administration of TAT-p27 represses cardiomyocyte apoptosis dependent on the autophagy process. (**A, B**). Expression of apoptosis-related proteins in preconditioned cardiomyocytes with TAT-p27. Representative figures (**A**) and quantitative analyses (**B**) of immunoblot assays demonstrate the expression of caspase-3 and caspase-8. The administration of bafilomycin A1 (BA1), 3-methyladenine (3-ME), and chloroquine (autophagy inhibitors) was used to prove the involvement of autophagy in the anti-apoptotic effects of p27. (**C, D**) Representative figures of TUNEL staining in the preconditioned cardiomyocytes using TAT-p27 (**C**) and quantitative analyses (**D**). The green fluorescence represents TUNEL-positive LPS-induced cardiomyocytes. The experiments were replicated 3 times. Data are presented as the mean  $\pm$ SD. \*\*  $P < 0.01$ , \*  $P < 0.05$ . TUNEL – terminal deoxynucleotidyl transferase dUTP nick end labeling.

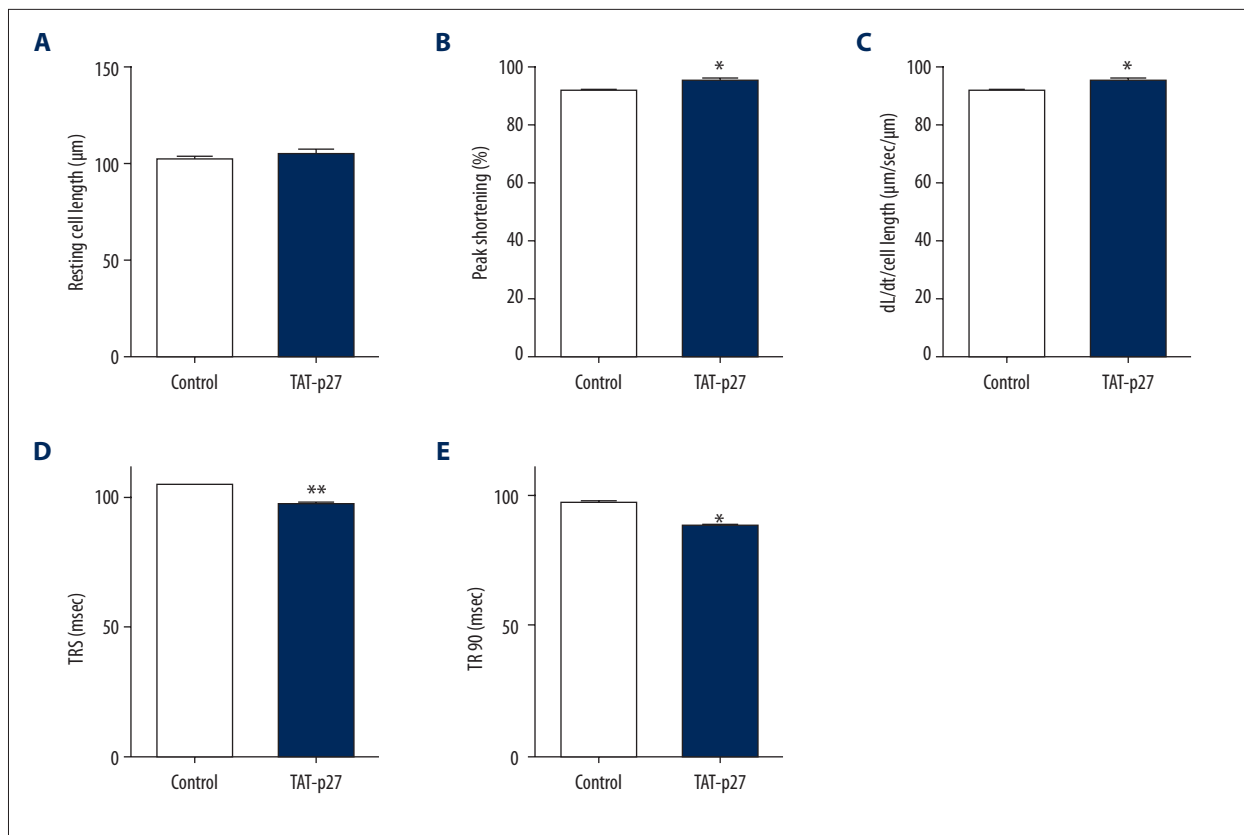


**Figure 3.** p27 improves cardiac mechanical contractile functions after treatment with LPS. LPS-induced cardiomyocyte contractile properties from Wistar rats treated with control and TAT-p27: (A) Resting cell length; (B) peak shortening (PS, normalized to cell length); (C) maximal velocity of shortening (+dL/dt); (D) time-to-PS (TPS); and (E) time-to-90% re-lengthening (TR90). Data are presented as the mean  $\pm$ SD, n=100 to 120 cells induced by LPS from 4 Wistar rats per group. \*\*  $P < 0.01$ , \*  $P < 0.05$  versus control. LPS – lipopolysaccharide.

peak shortening (PS) and maximal velocity of shortening/re-lengthening in primary cultured cardiomyocytes pretreated with LPS (Figure 3B, 3C). The time-to-PS and time-to-90% re-lengthening (TR90) were also increased in cardiomyocytes treated with TAT-p27 and infected with AAV9-p27, compared to controls (Figure 3D, 3E). Intriguingly, the autophagy inhibitors aforementioned abolished the improvements in cardiac mechanical properties due to the introduction of p27. These findings suggest that p27 improved cardiac mechanical properties and contractile functions via the activation of autophagy in LPS-stimulated cardiomyocytes.

### The protective effect of exogenous p27 was lost after the silencing of *Atg5* with siRNAs in LPS-induced cardiomyocytes

To reliably verify that autophagy is indispensable for the protective effect of p27 in cardiomyocytes induced with LPS due to the non-specificity of the autophagy inhibitors, we silenced *Atg5*, an essential gene for the formation of autophagosomes [26,27], to block autophagic flux and measured apoptosis after treatment

with exogenous p27. We found an increase in the levels of apoptosis-related proteins and a greater number of TUNEL-positive nuclei in *Atg5*-silenced cardiomyocytes (Figure 4A, 4B), which demonstrated that the loss of *Atg5* abrogated the protection by p27 in cardiomyocytes. As for cardiac mechanical contractile functions, we performed an assessment of mechanical properties and also found that the inhibition of autophagy repressed the improvement in mechanical contractile functions. We observed reduced PS and maximal velocity of shortening/re-lengthening in LPS-induced cardiomyocytes with *Atg5* silencing compared to only the introduction of p27 (Figure 4C, 4D). A similar change also occurred in other contractile function parameters, including time-to-PS and TR90 re-lengthening (Figure 4E, 4F). The block in autophagy impaired cardiac contractile functions and increased apoptosis by LPS stimulation in our study. These results showed that autophagy was important for the protective effects of p27, and that a direct inhibition of autophagy diminished the anti-apoptotic effects and improvements of mechanical properties attributed to the introduction of p27 in LPS-induced cardiomyocytes.

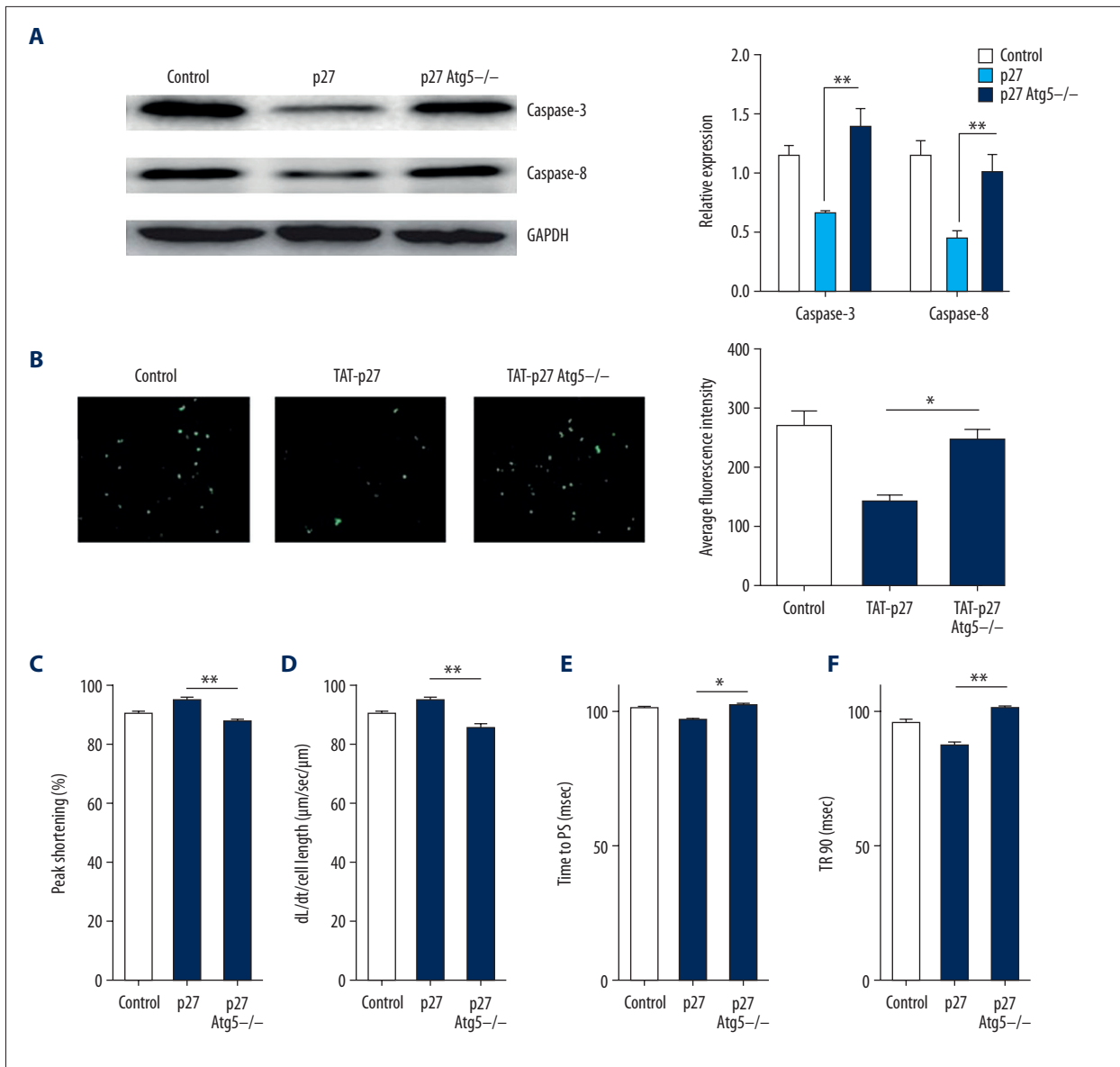


**Figure 4.** The protective effect of exogenous p27 fusion protein disappears after transfection with *Atg5*-siRNAs in LPS-induced cardiomyocytes. **(A)** Representative figures and quantitative analyses of western blots reflect the expression of caspase-3 and caspase-8 in LPS-induced cardiomyocytes preconditioned with TAT-p27 in different groups, including control, TAT-p27, and *Atg5*-silenced + TAT-p27 groups. **(B)** Representative figures of TUNEL staining in preconditioned cardiomyocytes and quantitative analyses in different groups, including control, TAT-p27, and *Atg5*-silenced + TAT-p27 groups. **(C–F)** Cardiomyocyte contractile properties among control, TAT-p27, and *Atg5*-silenced + TAT-p27 groups: **(C)** Peak shortening (PS, normalized to cell length); **(D)** Maximal velocity of shortening (+dL/dt); **(E)** Time-to-PS (TPS); and **(F)** Time-to-90% re-lengthening (TR90). The experiments were replicated 3 times. Data are presented as the mean  $\pm$ SD. \*\*  $P < 0.01$ , \*  $P < 0.05$ . TUNEL – terminal deoxynucleotidyl transferase dUTP nick end labeling.

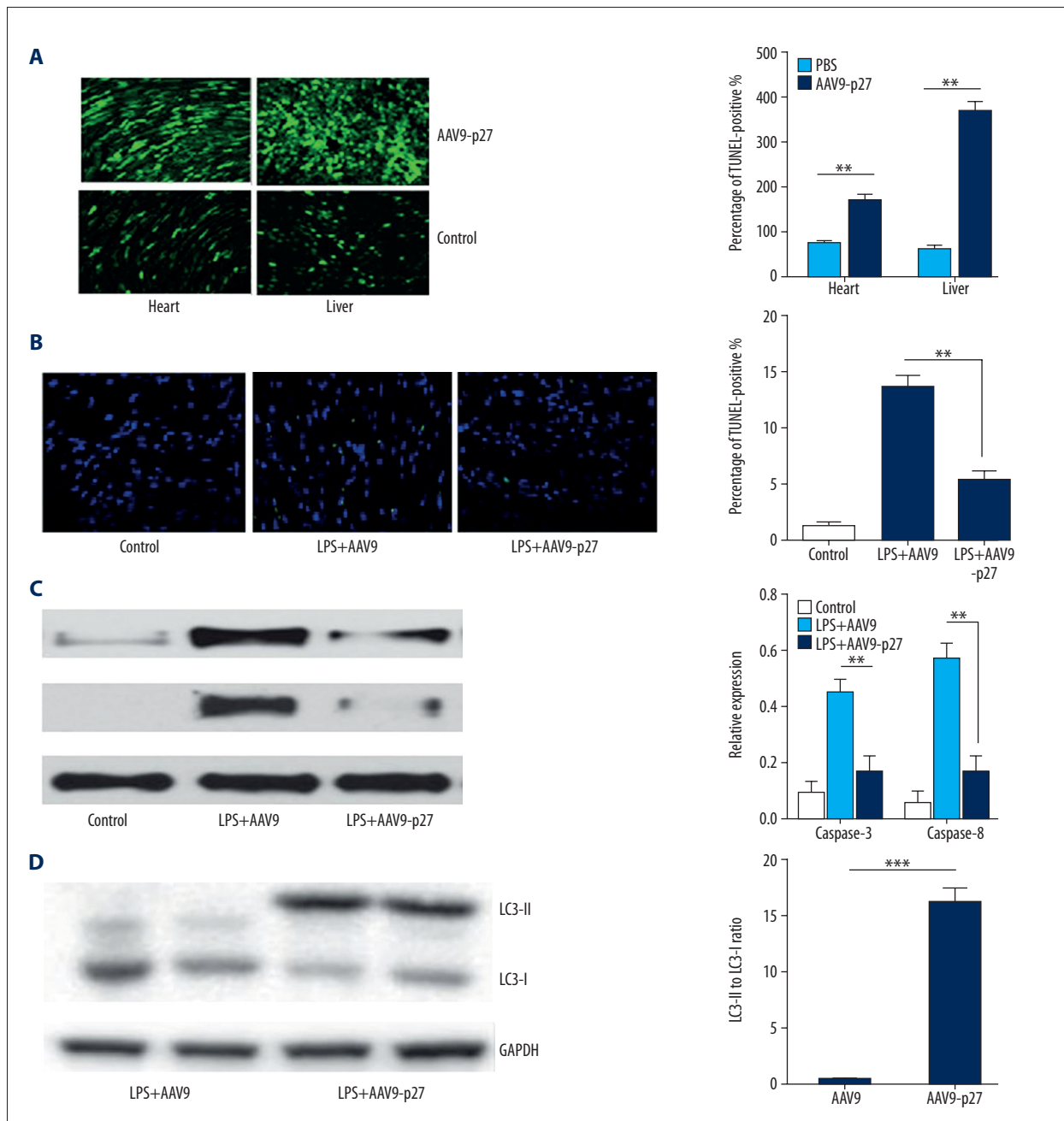
### p27 inhibited cardiomyocyte apoptosis and improved cardiac function in septic animal models via activation of autophagy *in vivo*

To identify the anti-apoptosis effect of p27 and the effect of p27 on cardiac function in septic animal models, we performed

intravenous injections of AAV9 viruses to achieve a partially specific transfection and overexpression of p27 in cardiac tissue. The efficiency of transfection was assessed by first visualizing the GFP marker by fluorescence microscopy to localize the intramyocardial overexpression of p27 (Figure 5A). We then detected apoptosis in septic rats infected with AAV9-p27 and

AAV9-control by TUNEL nuclear staining and western blotting. We found that the transfection of AAV9-p27 reduced cardiomyocytes apoptosis based on the lower frequency of TUNEL-positive nuclei compared to the control group (Figure 5B). A reduced expression of cleaved caspase-3 and caspase-8 was also detected in rats with a partially specific transfection of AAV9-p27 along with enhanced expression of LC3-II and an increased LC3-II/LC3-I ratio (Figure 5C, 5D). These data demonstrated that p27 inhibited apoptosis and activated autophagy in septic animals, consistent with the results from the *in vitro* experiments. Furthermore, we measured cardiac structure and

function 14 days after the CLP operation. We subsequently found an increased left ventricular ejection fraction and fractional shortening in septic rats transfected with AAV9-p27 compared to the control rats, but the left ventricular internal diastolic diameter showed no differences between the groups, which demonstrated that the overexpression of p27 in the heart improved cardiac systolic function but did not alter the slight adverse remodeling in septic models (Figure 5E, 5F). These results demonstrate the protective effects of p27 in septic animals and that the overexpression of p27 indeed improved cardiac function *in vivo*.



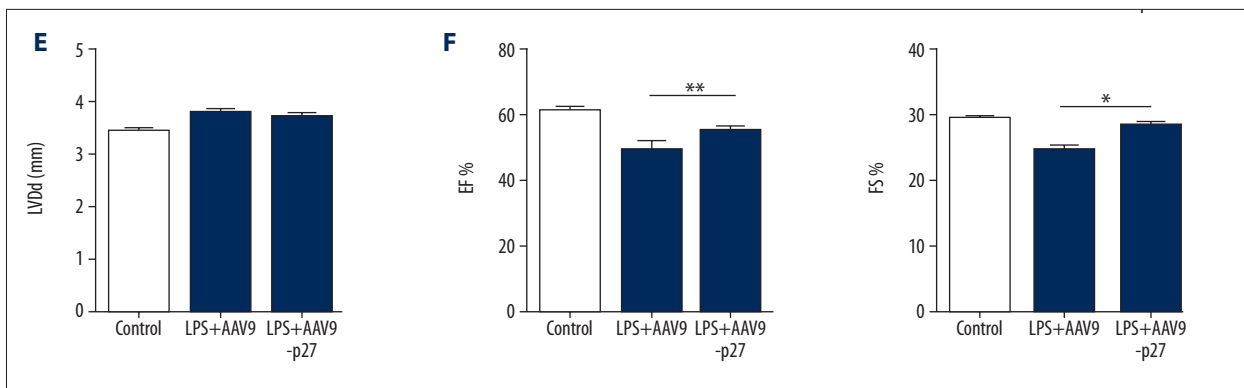


**Figure 5.** p27 inhibits cardiomyocyte apoptosis and improves cardiac function in septic animal models via the activation of autophagy *in vivo*. **(A)** Result of immunofluorescent assays of GFP in heart tissues of septic Wistar rats after tail vein injections of AAV9-p27 and isovolumetric PBS medium (n=5). **(B)** Representative figures of TUNEL staining in heart tissues from septic rats and quantitative analyses among control, empty vector, and AAV9-p27 groups (n=6). **(C)** The expression of apoptosis-related proteins in heart tissues from septic Wistar rats measured by western blot. The representative figures and quantitative analyses of immunoblot assays present, respectively, the expression of caspase-3 and caspase-8 among the different treated groups (n=6). **(D)** The expression of LC3-II and the ratio of the relative expression of LC3-II to LC3-I (GAPDH used as the reference protein) in heart tissues from septic rats treated with empty AAV9 vector or AAV9-p27 (n=6). **(E, F)** Cardiac size and cardiac systolic function: **(E)** left ventricular diastolic diameter; **(F)** left ventricular ejection fraction and fractional shorting (n=6). Data are presented as the mean  $\pm$  SD. The Student's *t*-test was used for the statistical analysis. \*\*  $P < 0.01$ , \*  $P < 0.05$ . GFP – green fluorescent protein; PBS – phosphate buffered saline; TUNEL – terminal deoxynucleotidyl transferase dUTP nick end labeling; AAV9 – adeno-associated virus serotype 9.

## Discussion

The presence of cardiac dysfunctions in sepsis results in increased mortality and a poor prognosis, and septic cardiac dysfunctions could lead to the occurrence of hemodynamic disorders and even septic shock. The precise mechanism of septic cardiac dysfunction remains unclear [9,10]. Some pathophysiological factors are considered to be involved in cardiac contractile dysfunction, including lipid peroxidation and free oxygen radical injuries, activation of a cascade of inflammatory response via LPS and its binding to TLR4, high concentrations of nitric oxide, regional ischemia, and activation of the coagulation process [28,29]. In recent years, several novel mechanisms have emerged after further research into septic cardiac depression. In the early stages of sepsis, high autophagy was activated but was followed by a decreased phase with impaired autophagy function. A significant decrease in the expression of LC3-II and an impaired autophagic flux in sepsis were observed [24,30]. The application of rapamycin reversed the impaired autophagy, improved the left ventricular ejection fraction suppressed apoptosis in septic models. Several groups assumed that inadequate autophagy may be one of the adverse factors in septic animal models and patients because the protective effects of autophagy have been shown in other organ dysfunctions and failures, including acute lung injury and acute renal failure, by meditating the programmed cell death pathway [31,32].

In metabolically stressed conditions, autophagy promotes cell survival as an evolutionally conserved mechanism related to environmental adaption [33]. In pressure load-induced heart failure, the activation of autophagy protected cardiomyocytes from apoptosis and improved cardiac function, but *Atg5* deletion deteriorated cardiac hypertrophy with impaired cardiac function [19]. Autophagy also inhibited myocardial ischemia/reperfusion (I/R) injury and improved the cell survival of I/R stressed cardiomyocytes in the border zone, which demonstrated that autophagy served as a conventional mechanism to improve cardiomyocyte survival in stressed conditions [20]. In the terminal stage of dilated cardiomyopathy, the dysfunction of autophagy might be a possible adverse factor for the survival of cardiomyocytes [34]. These studies all suggested that autophagy may be beneficial to protect cardiomyocytes from programmed cell death and improve cardiac function in septic cardiac depression and LPS-induced cardiomyocyte injury, the effect of autophagy has been gradually verified by several investigations [13]. LPS-induced oxidation was inhibited after the activation of autophagy by rapamycin, and subsequently, the cardiomyocytes were protected from increased reactive oxygen production and peroxidative damage [14]. Zou X et al. found that endoplasmic reticulum stress promoted the activation of autophagy in LPS-induced HL-1 cardiomyocytes and inhibited cellular apoptosis [13]. The 2 studies aforementioned demonstrated that autophagy not only has a positive influence on various stressed pathological conditions but also in mimetic septic cardiac depression models of cultured cardiomyocytes.

In recent years, studies have shown that p27Kip1, which serves as a key gatekeeper and regulator for the specific entrance to the cell cycle, plays a role in other important biological processes, including autophagy and cell differentiation [1–3]. The LKB1-AMPK pathway directly regulates the phosphorylation of the downstream factor p27 to enhance its stability, and induces autophagy to facilitate cell survival under low nutrient conditions, suggesting that p27 promotes autophagy and improves cell survival when cells are exposed to adverse conditions [7]. A subsequent study further showed that in cardiomyocytes suffering from glucose deprivation, p27 protected cells from apoptosis via the enhancement of autophagy [8]. Cardiac overexpression of p27 improved cardiac function, but the inhibition of autophagy abrogated this improvement, which proved that p27 protected cardiomyocytes from apoptosis when suffering from environmental stresses both *in vitro* and *in vivo*. These studies further verified the widespread involvement of p27 in crucial biological mechanisms beyond the regulation of the cell cycle and cell proliferation.

## Conclusions

In our study, as well according to previous studies aforementioned, we hypothesized that p27 activates autophagy to protect primary cardiomyocytes isolated from neonatal rats, when treated by LPS to imitate septic cardiac injury. We

analyzed the levels of LC3-II expression to assess the levels of autophagic flux and evaluated cell apoptosis after treatment with a p27 fusion protein. Our results were in line with research in metabolically stressed conditions, and suggest that p27 upregulates the activation of autophagy and inhibits apoptosis due to adverse environmental factors, as observed in previous studies. In addition, we evaluated the mechanical properties of LPS-induced cardiomyocytes. Surprisingly, we found that p27-induced autophagy improved cardiomyocyte mechanical properties, which was not consistent with a previous study showing that metallothionein (MT) improved cardiac contractile functions via the alleviation of oxidative damage and inhibition of endoplasmic reticulum stress without a correlation to autophagy. Our study found that p27 did indeed improve mechanical properties dependent on the activation of autophagy, which may be attributed to the fact that we directly activated autophagy by the introduction of p27, while metallothionein did not activate autophagy but rather inhibited other adverse biological mechanisms involved in cardiac function. In conclusion, our study demonstrated that p27 improved cardiac functions and protected cardiomyocytes dependent on the activation of autophagy and provides a novel potential therapeutic target in septic cardiac depression.

## Conflict of interests

None.

## References:

1. Bencivenga D, Caldarelli I, Stampone E et al: p27(Kip1) and human cancers: A reappraisal of a still enigmatic protein. *Cancer Lett*, 2017; 403: 354–65
2. Kaldis P: Another piece of the p27Kip1 puzzle. *Cell*, 2007; 128: 241–44
3. Sharma SS, Pledger WJ: The non-canonical functions of p27(Kip1) in normal and tumor biology. *Cell Cycle*, 2016; 15: 1189–201
4. Roy A, Banerjee S: p27 and leukemia: Cell cycle and beyond. *J Cell Physiol*, 2015; 230: 504–9
5. Drullion C, Tregoeat C, Lagarde V et al: Apoptosis and autophagy have opposite roles on imatinib-induced K562 leukemia cell senescence. *Cell Death Dis*, 2012; 3: e373
6. Jia W, He MX, McLeod IX et al: Autophagy regulates T lymphocyte proliferation through selective degradation of the cell-cycle inhibitor CDKN1B/p27Kip1. *Autophagy*, 2015; 11: 2335–45
7. Liang J, Shao SH, Xu ZX et al: The energy sensing LKB1-AMPK pathway regulates p27(kip1) phosphorylation mediating the decision to enter autophagy or apoptosis. *Nat Cell Biol*, 2007; 9: 218–24
8. Sun X, Momen A, Wu J et al: p27 protein protects metabolically stressed cardiomyocytes from apoptosis by promoting autophagy. *J Biol Chem*, 2014; 289: 16924–35
9. Takasu O, Gaut JP, Watanabe E et al: Mechanisms of cardiac and renal dysfunction in patients dying of sepsis. *Am J Respir Crit Care Med*, 2013; 187: 509–17
10. Sluijter JP, Doevendans PA: Sepsis-associated cardiac dysfunction is controlled by small RNA molecules. *J Mol Cell Cardiol*, 2016; 97: 67–69
11. Dellinger RP, Levy MM, Rhodes A et al: Surviving sepsis campaign: international guidelines for management of severe sepsis and septic shock: 2012. *Crit Care Med*, 2013; 41: 580–637
12. Yuan H, Perry CN, Huang C et al: LPS-induced autophagy is mediated by oxidative signaling in cardiomyocytes and is associated with cytoprotection. *Am J Physiol Heart Circ Physiol*, 2009; 296: H470–79
13. Zou X, Xu J, Yao S et al: Endoplasmic reticulum stress-mediated autophagy protects against lipopolysaccharide-induced apoptosis in HL-1 cardiomyocytes. *Exp Physiol*, 2014; 99: 1348–58
14. Hsieh CH, Pai PY, Hsueh HW et al: Complete induction of autophagy is essential for cardioprotection in sepsis. *Ann Surg*, 2011; 253: 1190–200
15. Alvarez S, Vico T, Vanasco V: Cardiac dysfunction, mitochondrial architecture, energy production, and inflammatory pathways: Interrelated aspects in endotoxemia and sepsis. *Int J Biochem Cell Biol*, 2016; 81: 307–14
16. Vandergriff AC, Hensley MT, Cheng K: Isolation and cryopreservation of neonatal rat cardiomyocytes. *J Vis Exp*, 2015; 117: 161–69
17. Zhao WY, Zhang L, Sui MX et al: Protective effects of sirtuin 3 in a murine model of sepsis-induced acute kidney injury. *Sci Rep*, 2016; 6: 33201
18. Ceylan-Isik AF, Zhao P, Zhang B et al: Cardiac overexpression of metallothionein rescues cardiac contractile dysfunction and endoplasmic reticulum stress but not autophagy in sepsis. *J Mol Cell Cardiol*, 2010; 48: 367–78
19. Su M, Wang J, Wang C et al: MicroRNA-221 inhibits autophagy and promotes heart failure by modulating the p27/CDK2/mTOR axis. *Cell Death Differ*, 2015; 22: 986–99
20. Xie M, Kong Y, Tan W et al: Histone deacetylase inhibition blunts ischemia/reperfusion injury by inducing cardiomyocyte autophagy. *Circulation*, 2014; 129: 1139–51
21. Rifki OF, Hill JA: Cardiac autophagy: Good with the bad. *J Cardiovasc Pharmacol*, 2012; 60: 248–52
22. Wu X, He L, Chen F et al: Impaired autophagy contributes to adverse cardiac remodeling in acute myocardial infarction. *PLoS One*, 2014; 9: e112891
23. Nakai A, Yamaguchi O, Takeda T et al: The role of autophagy in cardiomyocytes in the basal state and in response to hemodynamic stress. *Nat Med*, 2007; 13: 619–24
24. Ho J, Yu J, Wong SH et al: Autophagy in sepsis: Degradation into exhaustion? *Autophagy*, 2016; 12: 1073–82

25. Zang QS, Wolf SE, Minei JP: Sepsis-induced cardiac mitochondrial damage and potential therapeutic interventions in the elderly. *Aging Dis*, 2014; 5: 137–49
26. Noda NN, Inagaki F: Mechanisms of autophagy. *Annu Rev Biophys*, 2015; 44: 101–22
27. Rogov V, Dotsch V, Johansen T, Kirkin V: Interactions between autophagy receptors and ubiquitin-like proteins form the molecular basis for selective autophagy. *Mol Cell*, 2014; 53: 167–78
28. Baliya TM, Lowry SF: Lipopolysaccharide and sepsis-associated myocardial dysfunction. *Curr Opin Infect Dis*, 2011; 24: 248–53
29. Walley KR: Deeper understanding of mechanisms contributing to sepsis-induced myocardial dysfunction. *Crit Care*, 2014; 18: 137
30. Hsiao HW, Tsai KL, Wang LF et al: The decline of autophagy contributes to proximal tubular dysfunction during sepsis. *Shock*, 2012; 37: 289–96
31. Yen YT, Yang HR, Lo HC et al: Enhancing autophagy with activated protein C and rapamycin protects against sepsis-induced acute lung injury. *Surgery*, 2013; 153: 689–98
32. Jiang M, Wei Q, Dong G et al: Autophagy in proximal tubules protects against acute kidney injury. *Kidney Int*, 2012; 82: 1271–83
33. Lim YM, Lim H, Hur KY et al: Systemic autophagy insufficiency compromises adaptation to metabolic stress and facilitates progression from obesity to diabetes. *Nat Commun*, 2014; 5: 4934
34. Muhammad E, Levitas A, Singh SR et al: PLEKHM2 mutation leads to abnormal localization of lysosomes, impaired autophagy flux and associates with recessive dilated cardiomyopathy and left ventricular noncompaction. *Hum Mol Genet*, 2015; 24: 7227–40